

# Contemporary statistical inference for infectious disease models using Stan

Anastasia Chatzilena<sup>a</sup>, Edwin van Leeuwen<sup>b</sup>, Oliver Ratmann<sup>c</sup>, Marc Baguelin<sup>d,e</sup>, Nikolaos Demiris<sup>f,g</sup>

<sup>a</sup>*Department of Economics, Athens University of Economics and Business, Athens, Greece*

<sup>b</sup>*Respiratory Diseases Department, Public Health England, London, United Kingdom*

<sup>c</sup>*Department of Mathematics, Imperial College London, United Kingdom*

<sup>d</sup>*School of Public Health, Infectious Disease Epidemiology, Imperial College London, United Kingdom*

<sup>e</sup>*Centre for Mathematical Modelling of Infectious Disease and Department of Infectious Disease Epidemiology, London School of Hygiene and Tropical Medicine, London, UK*

<sup>f</sup>*Department of Statistics, Athens University of Economics and Business, Athens, Greece*

<sup>g</sup>*Cambridge Clinical Trials Unit, University of Cambridge, Cambridge, UK*

---

## Abstract

This paper is concerned with the application of recently developed statistical methods for inference in infectious disease models. We use hierarchical models as well as deterministic and stochastic epidemic processes based upon systems of ordinary differential equations. We illustrate the application of Hamiltonian Monte Carlo and Variational Inference using the freely available software Stan. The methods are applied to real data from outbreaks as well as routinely collected observations. The results suggest that both inference methods are feasible in this context and show a trade-off between statistical efficiency versus computational speed. The latter appears particularly relevant for real-time applications.

*Keywords:* Hamiltonian Monte Carlo, Automatic Differentiation Variational Inference, Stan, epidemic models

---

## 1. Introduction

One of the most crucial steps in epidemiology is the estimation of model parameters describing the mechanisms of disease spread. Inference for epidemic models is complicated by the fact that one or several of the model

variables may be unobserved (latent). To this end, employing a Bayesian approach has the advantage of including uncertainties within the model. The Bayesian approach to practical applications of statistics has exploded since the introduction of Markov chain Monte Carlo (MCMC) methods with the use of MCMC in practical applications being greatly facilitated by the early development of the BUGS software (Lunn et al., 2000). Most of the recent studies in infectious disease epidemiology use MCMC and adaptive MCMC for learning the model parameters from data (Baguelin et al., 2013; McKinley et al., 2014; O'Neill and Roberts, 1999).

As model complexity increases, the performance of classical MCMC algorithms deteriorates due to their potentially limited exploration of the target distribution. The latest developments in statistics and machine learning suggest that Hamiltonian Monte Carlo (HMC) methods (Betancourt, 2017; Neal, 2012) and Variational Bayes (VB) (Blei et al., 2017; Kucukelbir et al., 2017) can offer statistical and/or computational efficiency compared to MCMC. While there have been a number of successors to the BUGS software, especially over the last decade, including JAGS (Plummer, 2017) and Nimble (de Valpine et al., 2017), a relatively new software package called Stan (Carpenter et al., 2017; Stan Development Team, 2018) enables the implementation of both HMC and VB within a probabilistic modeling language. In addition, it appears that Stan is the first such software which has built-in solvers for systems of ordinary differential equations (ODEs). However, their potential has not been hitherto explored for learning parameters of epidemic models.

Our main purpose in this paper is to provide a brief description of the most important features of Stan's implementation of HMC and VB in the context of epidemic models. In particular, we employ an example of a hierarchical model examining the age-specific gonorrhoea diagnosis rates after adjusting for spatial heterogeneity, as well as models based upon ODE systems describing the transmission dynamics of a single or multiple strains of influenza. The methods are applied to both outbreak and routinely collected epidemic data. All code used is made freely available in [https://github.com/anastasiachtz/COMMAND\\_stan.git](https://github.com/anastasiachtz/COMMAND_stan.git).

## 2. Statistical inference using Stan

Stan is open-source general purpose inference software, which implements full Bayesian inference with gradient based sampling techniques, a method to

approximate posteriors with variational inference as well as penalized maximum likelihood estimation via optimization. The software performs the required computations using advanced techniques such as automatic differentiation (Griewank and Walther, 2008; Griewank et al., 1989) and No-U-turn Sampler(NUTS) (Hoffman and Gelman, 2011). Moreover, Stan is one of the few general purpose software which provides a built-in mechanism for specifying and solving systems of ordinary differential equations which makes it suitable for inference in epidemic models.

The user can write a Bayesian model in a BUGS-like language which is similar to standard statistical notation. The model is then compiled to C++, making the inference faster. A difference between Stan code and other automated platforms such as BUGS and JAGS, is the necessary variable type declarations and statements. Variables are declared by their type, in blocks according to their use, and constraints upon them need to be defined carefully. The first blocks of Stan’s model statement consist of data, transformed data, parameters, transformed parameters and generated quantities. Within the model block, sampling notation is very similar to BUGS. Log probability variables can also be accessed directly, or user-defined probability functions can be employed. The Stan model file should have the extension `.stan` and is portable across the different interfaces. There are interfaces for R, Python, MATLAB, Julia, Stata, Mathematica, Scala and the command line. According to the interface used, the user needs to call a different function for the different inference methods offered. All these functions include an argument which defines the location and name of the Stan model file.

Stan is the only platform that currently implements HMC and Automatic Differentiation Variational Inference (ADVI) (Kucukelbir et al., 2015) as an integral part of the package. Moreover, extensive diagnostics for the inference are provided. In the following section we highlight the basic concepts of HMC and ADVI focusing on the way they are implemented in Stan. A more detailed mathematical description of the algorithms is included in the Appendix.

### *2.1. Hamiltonian Monte Carlo*

A commonly used method in statistical inference for epidemic models is MCMC. MCMC consists of a whole range of algorithms for sampling from probability distributions by generating a Markov chain that has the target distribution as its stationary distribution. The idea behind classical MCMC techniques such as the Metropolis-Hasting algorithm (Hastings, 1970;

Metropolis et al., 1953) and Gibbs sampling (Geman and Geman, 1984) is to explore parameter space by proposing a new sample based on the current state and then accept or reject it according to a given probability. In challenging problems the algorithm cannot jump between regions of the parameter space which are distant from the current state. Thus, even though eventually it may manage to explore all the regions, this can require exceedingly long runs. The resulting slow exploration will produce large autocorrelations and slow mixing (Hoffman and Gelman, 2011; Neal, 1993) which are hard to cope with in the finite time available in a real analysis.

In contrast, instead of exploring the parameter space using random uninformed jumps, HMC defines the direction in which the posterior density will move in a way that is determined by the gradient using Hamiltonian dynamics and defines the proposed move accordingly (Neal, 2012). The theoretical foundation of HMC is formulated in terms of differential geometry (Betancourt et al., 2017) which is out of the scope of this paper but in order to understand the intuition behind the method we will illustrate its basic steps. At first, auxiliary momentum parameters are introduced in addition to the parameters of interest and upon the joint density of all the parameters, the Hamiltonian function is formulated. Then the momentum parameters are sampled, typically from their Gaussian distribution, given the current values of the parameters of interest and the proposal is designed based on the gradients of the Hamiltonian. More specifically, most HMC implementations, including Stan, use the leapfrog method alternating between half-step updates of the momentum parameters and full steps of the parameters of interest. Since most of the times analytic gradients of the posterior are not available and we have to approximate them numerically, Stan uses automatic differentiation<sup>1</sup> (Carpenter et al., 2015; Griewank and Walther, 2008). Finally, an acceptance step accounting for the approximation of the Hamiltonian ensures that the resulting samples are asymptotically from the target posterior density.

The number of updates performed, and the size of each update are parameters which need to be tuned for the algorithm to be efficient (Betancourt, 2016; Betancourt et al., 2014). Also, the probability distribution of the mo-

---

<sup>1</sup>Automatic differentiation, instead of computing the expressions of the derivatives, decomposes the complex expressions into primitive ones and computes the derivatives through accumulation of values during code execution, resulting in numerical derivatives.

momentum parameters involves a covariance matrix which needs to be specified. All the aforementioned concerns make the implementation of HMC an intricate problem. However, advanced platforms like Stan simplify these burdens using an adaptive form of HMC. Stan estimates the covariance matrix during warm-up and uses NUTS to decide on the optimal number of steps and their length. The idea behind NUTS is to use enough steps to explore the parameter space properly but not too many ending up with samples too similar to one another. So the sampling algorithm stops automatically, determining the number of steps, when the designed path turns around in the sense that it reaches already sampled points. Finally, the step size is determined during warm-up in order to achieve a target acceptance rate which is also the only remaining tuning parameter (Stan Development Team, 2018).

Even though it is obvious that HMC requires more computational effort at every step compared to classical MCMC techniques, it explores the target distribution more effectively, especially in the case of highly correlated posterior distributions.

## *2.2. Variational Inference*

There are real-life applications in statistics where we cannot easily use the MCMC approach due to time constraints. This may be relevant when repeated fitting is required but is especially pressing in epidemic analysis where real-time inference may be the object of interest. In these cases, we may be willing to partially sacrifice accuracy for computational speed. Variational inference is a method which originates from machine learning and tends to be faster than MCMC (Jordan et al., 1999; Wainwright et al., 2008). Its core relies on translating the problem of the computation of the posterior distribution into an optimization problem trying to find a density close to the target. More formally, variational inference considers a family of approximations to the exact posterior distribution. Each member of this family is a candidate approximation to the exact posterior density and the goal is to find the closest candidate in Kullback-Leibler(KL) divergence to the exact density (Blei et al., 2017). However, the KL divergence is not computable because it involves the posterior. For this reason, variational inference maximizes a proxy to the KL divergence, the Evidence Lower Bound (ELBO).

Stan implements an automatic variational inference method, called automatic differentiation variational inference (ADVI). The fact that we need to optimize the KL divergence, implies a constraint that the support of the chosen approximation lies within the support of the posterior(Kucukelbir et al.,

2015), but finding such a family of approximating densities is very difficult. To overcome this challenge, ADVI transforms the support of the parameters of interest to the real coordinate space, ensuring that the aforementioned constraint is always valid. Then all the unobserved parameters are defined on the same space and we can choose the variational approximation independent of the model. To this end, Stan provides a library of transformations. Considering then a Gaussian variational approximation, ADVI tries to maximize the ELBO. Of course, the variational approximation in the original parameter space is non-Gaussian and its shape is directly tied to the form of the transformation used. In contrast to variational inference which maximizes the ELBO using coordinate ascent, ADVI uses a gradient-based algorithm to perform the maximization. In particular, ADVI is based on a stochastic gradient ascent algorithm that uses automatic differentiation to compute gradients and Monte Carlo integration to approximate expectations (Kucukelbir et al., 2015).

Stan offers two options for the Gaussian approximation used. The first one is the mean-field variant which employs a factorized Gaussian variational approximation to the posterior. The mean field variational Bayes is widely used since it is fast, however it does not guarantee accurate results (Wang and Blei, 2018) and it often underestimates marginal variances (Bishop, 2006; Turner and Sahani, 2011). The other option is a non-factorizing version of ADVI, which is called full-rank and is more suitable for capturing posterior correlations.

Despite the fact that ADVI in Stan is a faster alternative and is automated in the sense that the user needs to provide only the model and data, it may fail for several reasons. As in every variational inference approach, initialization plays a crucial role and we can only test random initializations. Also, the fact that the posterior in the transformed space may not be well-approximated by a multivariate normal or that this specific iterative algorithm may not be able to find that optimal multivariate normal, may lead to poor performance.

### 3. Modelling

#### 3.1. Hierarchical Models

Heterogeneity is a common feature in infectious-disease epidemiology and medical statistics in general. Multiple subsets of patients, multiple treatment group contrasts, multiple cities or hospitals and multiple time points at which measurements are taken, may reflect the structure of the data and constitute

key points of the analysis. Also, the model itself may have multiple levels incorporating parameters controlled by hyperparameters (Gelman and Hill, 2006). Hierarchical models are the basic modeling tool in these cases. Stan was originally designed as an alternative general platform for Bayesian inference for multilevel models while trying to overcome difficulties arising from using BUGS or JAGS (Lunn et al., 2012; Plummer et al., 2003; Stan Development Team, 2018), but is often especially suited for hierarchical models.

In order to illustrate how Stan handles full hierarchical models, we will provide an example of estimation of diagnosis rates according to age, gender and geographic characteristics. However, incorporating both group- and individual-level parameters in the model results in challenging inference due to the many parameters for multiple units. The typical modelling assumptions employed are that the parameters can be identical, independent or exchangeable (Spiegelhalter et al., 2004). In particular, if we assume that the parameters are identical, the group or individual units are ignored, and all the data are pooled without incorporating possible variation between different units/groups. Assuming independence, we can specify a prior for each unit and make inference for each unit independently, ignoring any information coming from the other units. However, a weakness of this approach is that we examine one unit after the other and everything we learned from the previous units is forgotten, which precludes using information from one unit to inform the fitting of the other units. Finally, an intermediate approach is to assume exchangeable parameters or random-effects as they are termed, whence we treat the parameters of the different units as distinct but similar, drawn from the same distribution conditional on some unknown parameters. More formally, we specify a common prior for all units, with unknown parameters referred to as hyperparameters. Specifying priors for the hyperparameters results in a two-level hierarchical model which can reflect prior beliefs concerning possible variation between units. As a result, we use information from all units to improve the estimates of each individual unit (McElreath, 2016).

### *3.1.1. Poisson mixed model*

We consider surveillance data for gonorrhoea in England between 2012 and 2016 and build increasingly realistic models reflecting reality. Our aim is to characterize gonorrhoea diagnosis rates by age, gender and geographically

and for that purpose we employ a Poisson regression model:

$$y_{cas} \sim \text{Poisson}(\kappa_{cas}) \quad (1)$$

$$\log(\kappa_{cas}) = \alpha + \log(T_{cas}) + \beta_M \text{MALE}_{cas} \quad (2)$$

where  $y_{cas}$  is the number of gonorrhoea cases from Public Health England (PHE) centre  $c$ , age category  $a$  and sex  $s$ ,  $T_{cas}$  are the person-years of exposure time in centre  $c$ , and for age category  $a$  and sex  $s$  and  $\text{MALE}_{cas}$  is an indicator variable that evaluates to 1 if  $s$  is male and 0 if  $s$  is female.

In order to implement HMC we use Normal priors for both  $\alpha$  and  $\beta_M$ . However, if we plot crude diagnosis rate estimates of the above model for each region against the overall median posterior estimate and 95% credibility intervals, we notice that there is considerable heterogeneity in diagnosis rates across PHE centres, which is not reflected in the model. This motivates us to add sex-homogeneous random effects across PHE centres.

This model results in region-specific posterior medians which provide a good fit to the crude incidence estimates, but we still observe substantial variation in the crude incidence estimates for each region, which is not reflected in the model. Visualizing the trends in diagnosis rates by age, we observe that there is substantial heterogeneity by age category, which can be modelled through additional random effects. Also, diagnoses peak at younger age among women when compared to men, suggesting that separate age-specific random effects should be added for males and females. Finally, we notice that diagnoses among males from London are substantially higher and since the sample size in London is large, this is unlikely due to error. So, if this is not accounted for, the overall estimates will be biased upwards, thus we should add also an independent effect for London males to the model. All the above motivate the following model:

$$y_{cas} \sim \text{Poisson}(\kappa_{cas}) \quad (3)$$

$$\begin{aligned} \log(\kappa_{cas}) = & \alpha + \alpha_c + \xi_a * \text{MALE}_{cas} + \nu_a * (1 - \text{MALE}_{cas}) + \\ & \log(T_{cas}) + \beta_M \text{MALE}_{cas} + \beta_{ML} \text{MALE}_{cas} * \text{LONDON}_{cas} \end{aligned} \quad (4)$$

where  $\text{LONDON}_{cas}$  equals 1 if  $c$  is London, and 0 otherwise.

We assume Normal priors for the intercept and slope parameters:

$$\alpha \sim \mathcal{N}(0, 100)$$

$$\alpha_c \sim \mathcal{N}(0, \sigma_\alpha^2), \quad \xi_a \sim \mathcal{N}(0, \sigma_\xi^2), \quad \nu_a \sim \mathcal{N}(0, \sigma_\nu^2)$$

$$\beta_M \sim \mathcal{N}(0, 10), \quad \beta_{ML} \sim \mathcal{N}(0, 10)$$

and exponential priors for the variance parameters.

### 3.2. SIR/ODE-based models

Most of the transmission models in epidemiology are compartmental models, with the population being divided into compartments representing a specific stage of the epidemic or a demographic status (Kermack and McKendrick, 1927). The theoretical framework most commonly used contains susceptible, infected, and recovered individuals. When dealing with large populations, deterministic models may reasonably be used in which case the transition rates from one compartment to another are mathematically expressed as derivatives and these susceptible-infectious-recovered (SIR) models can be expressed as a system of non-linear ODEs (Anderson and May, 1992):

$$\begin{aligned}\frac{dS}{dt} &= -\beta \frac{I(t)}{N} S(t) \\ \frac{dI}{dt} &= \beta \frac{I(t)}{N} S(t) - \gamma I(t) \\ \frac{dR}{dt} &= \gamma I(t)\end{aligned}\tag{5}$$

where  $S(t)$  represents the number of susceptible,  $I(t)$  the number of infected and  $R(t)$  the number of recovered individuals at time  $t$ .  $N$  is the total population size ( $N = S(t) + I(t) + R(t)$ ),  $\beta$  is the transmission rate and  $\gamma$  is the recovery rate.

Inference for the parameters linking compartments is complicated by the fact that one or several of the model variables may be unobserved (latent) and the presence of a non-linear system of ODEs makes the estimation a difficult task. Along with these parameters, we usually want to obtain estimates of the initial number of susceptible individuals and the basic reproduction number  $R_0$  defined as the ratio  $\frac{\beta}{\gamma}$ . In this model it has a natural interpretation as the expected number of infections generated by one infectious individual in a large completely susceptible population. The basic reproduction number is a key quantity to transmission dynamics as it determines the critical proportion of individuals that has to be vaccinated in order to eliminate the disease (Dietz, 1993).

Stan has two built-in ODE solvers<sup>2</sup> which provide a user-friendly solution to this problem appearing in epidemic analysis. In particular, the first one which is suitable for non-stiff systems, uses fourth and fifth order Runge-Kutta method being relatively fast while the second one is designed to deal with stiff systems and even though it is slower, it is more robust (Stan Development Team, 2018).

In what follows, we provide a setting where the ODE solver role is highlighted in the context of an SIR model. We implement both HMC and ADVI at first in a deterministic setting and then adding stochasticity. Finally, we address a variant that models many strains independently.

### 3.2.1. Single strain deterministic and stochastic models

We examine an outbreak of influenza A (H1N1) in 1978 at a British boarding school. We use daily data on the number of students in bed, spanning over a time interval of 14 days. In the context of a deterministic SIR, in order to estimate the transmission and the recovery rate, we use two different specifications.

First, we assume that the total number of infected students each day  $Y_t$ , follows a Poisson distribution:

Model 1:

$$Y_t \sim \text{Poisson}(\lambda_t) \tag{6}$$

$$\lambda_t = \int_{t-1}^t \left( \beta \frac{I_s}{N} S_s - \gamma I_s \right) ds \tag{7}$$

In order to perform both HMC and ADVI, we use a log-normal prior for the transmission rate,  $\beta \sim \text{Lognormal}(0, 1)$  and assuming that the mean infectious period is 5 days we employ a Gamma prior for the recovery rate with  $\gamma \sim \Gamma(0.004, 0.002)$ . Finally, we use Jeffreys prior for the initial proportion of susceptible individuals,  $s(0) \sim \text{Beta}(0.5, 0.5)$ .

---

<sup>2</sup>Both solvers look like function applications, but they take specific arguments. The first argument must be the function that describes the ODE system but the other arguments, except for the initial state and the parameters, are restricted to data only expressions already declared. A system of ODEs is coded directly in Stan as a function with a strictly specified signature as well. It takes as input time, system state, parameters and real and integer data, in exactly this order, and returns the derivatives with respect to time. Note that, the initial state can also be estimated along with the parameters describing the system.

Using the same prior distributions, we also estimate a Binomial model, formulated as follows:

Model 2:

$$Y_t \sim \text{Bin}(N, p_t) \quad (8)$$

$$p_t = \int_{t-1}^t (\beta i_s s_s - \gamma i_s) ds \quad (9)$$

where  $s_s$  is the fraction of susceptible students and  $i_s$  is the fraction of infected students.

Even though the deterministic approach gives us an insight into the dynamics of the disease, adding stochasticity may allow for a more accurate estimation of the parameters related to the spread of the disease, as the stochastic component can absorb the noise generated by a possible mis-specification of the model (Andersson and Britton, 2000; Malesios et al., 2017). We are going to extend our Poisson model to include stochastic variation by incorporating an Ornstein-Uhlenbeck (OU) process as follows:

Model 3:

$$Y_t \sim \text{Poisson}(\lambda_t) \quad (10)$$

$$\lambda_t = \exp(\kappa_t) \quad (11)$$

$$d\kappa_s = \phi(\mu_t - \kappa_s)dt + \sigma dB_s, t-1 < s < t \quad (12)$$

where  $B_s$  denotes Standard Brownian motion,  $\sigma$  is the instantaneous diffusion term,  $\phi$  is the speed of reversion of  $\kappa_t$  and  $\mu_t$  is a piecewise constant function which corresponds to the logarithm of the solution of the deterministic model:

$$\mu_t = \log \left( \int_{t-1}^t \left( \beta \frac{I_s}{N} S_s - \gamma I_s \right) ds \right) \quad (13)$$

Thus, the instantaneous  $\kappa_t$  is an OU process evolving around  $\mu_t$  and its transition density is available in closed form, denoted as:

$$\kappa_{t+1}/\kappa_t \sim \mathcal{N} \left( \mu_t + (\kappa_t - \mu_t)e^{-\phi}, \frac{\sigma^2}{2\phi}(1 - e^{-2\phi}) \right) \quad (14)$$

We run both HMC and ADVI considering a half-normal prior distribution for  $\phi$  with large variance and an inverse-gamma posterior density for  $\sigma^2$ .

### 3.2.2. Multistrain deterministic models

In the previous example we were interested in a single strain of influenza, here we describe a model that models three different strains independently and using historic data we implement the model in Stan. The model used is based on a SIR model where each strain acts independently and it is fitted to both weekly influenza-like illness (ILI) and virological data.

Thus, the model is described by the following formulation:

$$\begin{aligned}\frac{dS_s}{dt} &= -\beta_s \frac{I_s(t)}{N} S_s(t) \\ \frac{dI_s}{dt} &= \beta_s \frac{I_s(t)}{N} S_s(t) - \gamma I_s(t) \\ \frac{dR_s}{dt} &= \gamma I_s(t)\end{aligned}\tag{15}$$

with  $S_s(t)$  representing the number of susceptibles at time  $t$  (in days) and for strain  $s$  and, similarly,  $I_s(t)$  and  $R_s(t)$  representing the number of infected and recovered at a certain time and for a certain strain.  $N$  is the total population size ( $N = S_s + I_s + R_s$ ),  $\beta_s$  is the strain specific rate of transmission and  $\gamma$  is the rate of recovery per day.

In order to monitor each strain, we track influenza caused ILI cases ( $\text{ILI}^{+,s}$ ) by strain ( $s$ ) and ILI cases that are not caused by influenza ( $\text{ILI}^-$ ). The total number of ILI cases can then be calculated with:  $\text{ILI} = \sum_s \text{ILI}^{+,s} + \text{ILI}^-$ .

Therefore,

$$\begin{aligned}\frac{d\text{ILI}^{+,s}}{dt} &= \theta_s^+ \beta_s \frac{I_s(t)}{N} S_s(t) - \text{ILI}^{+,s}(t) \delta(t \bmod 7) \\ \frac{d\text{ILI}^-}{dt} &= \theta^-(t) (N - \sum_s I_s(t)) - \text{ILI}^-(t) \delta(t \bmod 7)\end{aligned}\tag{16}$$

with  $\theta_s^+$  denoting the rate of becoming symptomatic due to flu and  $\theta^-$  the rate of developing ILI symptoms when not having flu.  $\delta(t \bmod 7)$  is the Dirac delta function, which causes both ILI states to reset to zero when  $t \bmod 7 = 0$ , i.e. every week.

It is well known that flu-negative ILI rates also increase during the winter (Fleming and Elliot, 2008). To account for this,  $\theta^-$  was assumed to change over time as follows:  $\log \theta^-(t) = \hat{\theta} + \phi \left( e^{-\frac{(t-\mu_t)^2}{2\sigma^2}} - 1 \right)$ , where  $\hat{\theta}$  is the maxi-

mum value of the (log) value of the flu negative ILI rate,  $\phi$  is the amplitude of the peak,  $\mu_t$  is the time of the peak and  $\sigma$  governs the width of the peak.

The general approach is to fit the monitored variables ( $ILI^{+,s}$  and  $ILI^-$ ) to the data. First we assume that the number of ILI has the following distribution:

$$\mathcal{L}(ILI; y^{ILI}, ILI, N, N_c, \epsilon) = \mathcal{B}(y^{ILI}; ILI N_c / N, \epsilon)$$

where,  $y_i^{ILI}$  is the measured number of ILI cases in the catchment population  $N_c$ ,  $N$  is the total population,  $ILI$  is the total predicted ILI cases in the population (see above) and  $\epsilon$  is the rate with which someone with ILI is diagnosed, i.e. this is a combination of the probability that the infected cases consult the GP and the GP correctly diagnosing the patient.

The virological samples are assumed to follow a multinomial distribution:

$$\mathcal{M}(y^{+,s_0}, \dots, y^-; ILI^{+,s_0}/ILI, \dots, ILI^-/ILI)$$

where  $y^{+,H1}, y^{+,H3}, y^{+,B}$  represent the number of positive samples for each strain,  $y^-$  is the number of negative samples and  $ILI^{+,s_0}/ILI, \dots, ILI^-/ILI$  are respectively the probability of finding positive samples with each strain  $s_0, \dots$  and finding negative samples (flu negative ILI).

## 4. Real data applications

### 4.1. Poisson mixed model

Gonorrhoea is a sexually transmitted bacterial infection with potential of becoming multi-drug resistant. In October 2015, a national resistance alert was issued as an outbreak of high-level azithromycin resistant gonorrhoea was detected in Leeds. From 2008 to 2015, new gonorrhoea diagnoses increased in England from 14,985 to 41,262 and then decreased to 36,244 in 2016. We use gonorrhoea case data from 9 PHE centres, from different age groups and sexes.

We fit our full hierarchical model as described by equations (3)-(4), using Stan's NUTS algorithm. A measure that helps us to monitor if the HMC has generated Markov chains that explore fast, is the effective sample size which is an estimate of the number of independent draws from the posterior distribution. The number of effective sample size metric used in Stan is based on the ability of the draws to estimate the true mean value of the

parameter. In this example, in order to obtain effective sample sizes above 500, approximately 30000 iterations are needed. Also, inspecting the trace plots for multiple chains suggests that there is no lack of convergence.

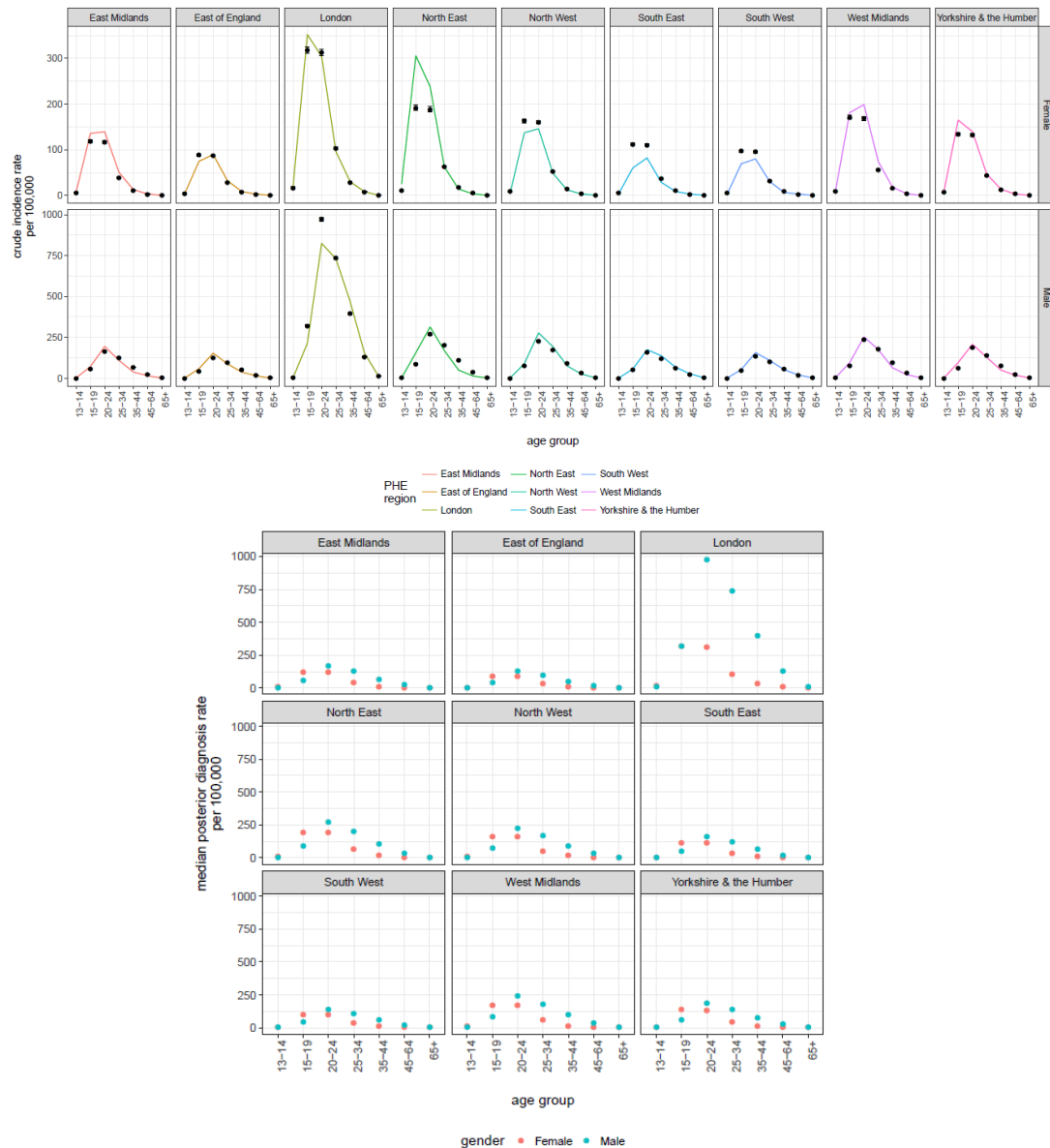


Figure 1: Model fit to the data using Hamiltonian Monte Carlo. Top panel has the age-and-region specific diagnosis rate estimates between males and females. The bottom panel has a comparison of the diagnosis rate estimates between males and females.

Overall, the model is fairly consistent with the case data in terms of trends by age and gender. The main shortcoming is that the 95% credibility intervals are too tight, which could be mitigated through a Poisson-Gamma overdispersion model. For some PHE centres however, the predictive distributions are far from the actual case data, e.g. females in South East and South West England (Figure 1).

In summary, the final age-specific model indicates that young women aged 15-19 have higher risk of acquiring gonorrhoea than their male peers. However, among all older age groups 20-64, it is the men that have higher risk of acquiring gonorrhoea when compared to their female peers as seen in Figure 1. We notice that, among females, young women aged 15-24 have atypically low diagnosis rates in the South East and South West, but atypically high diagnosis rates in the North East. Clearly, among men, all age groups in London have substantially higher risk of becoming diagnosed with gonorrhoea, interestingly though, crude diagnosis rates among London men aged 20-24 are lower than expected.

#### *4.2. Single strain SIR models*

In 1978, there was a report to the British Medical Journal for an influenza outbreak in a boarding school in the north of England. There were 763 male students which were mostly full boarders and 512 of them became ill. The outbreak lasted from the 22nd of January to the 4th of February and it is reported that one infected boy started the epidemic and then it spread rapidly in the relatively closed community of the boarding school. We use the data from Chapter 9 of De Vries et al. (2006) which are freely available in the R package outbreaks, maintained as part of the R Epidemics Consortium (RECON; <http://www.repidemicsconsortium.org>). Data consist of the number of bedridden students rather than the number of infected students, so we assume that the number of students who are confined to bed each day are those who are newly infected and all these who are still in bed after being infected on a prior day, consisting all together the total number of infected students each day.

All three models are fitted using Stan's NUTS algorithm using 5 chains, each with 100500 iterations of which the first 500 are warm-up to automatically tune the sampler, and then a sample is saved every fiftieth samples, leading to a total of 10000 posterior samples. We examine the convergence of the parameters by inspecting the trace plots of all chains indicating that

there is no lack of convergence for all models and by checking the  $\hat{R}$  convergence statistic reported by Stan. Therefore, if the chains have not yet converged to a common distribution the  $\hat{R}$  statistic will be greater than one (Gelman et al., 2013; Stan Development Team, 2018). However, if it is equal to 1, it does not necessarily indicate convergence. As all convergence diagnostics,  $\hat{R}$  can only detect failure to convergence but it cannot guarantee convergence. In our example, all models show good mixing according to the effective sample size,  $\hat{R}$  and the trace plots.

We also fit the models using the mean-field ADVI variant of Stan. All models were sensitive to initial values so we initialize our parameters using values drawn uniformly from the credible intervals we obtain from NUTS. In our example, the full-rank variant was not feasible.

For the deterministic setting, posterior medians and 95% credible intervals of the parameters are summarized in Table 1. Estimates of the Poisson model (Model 1) are very close to the estimates of the Binomial model (Model 2), irrespectively of the inference method used. In both models, ADVI results in narrower credible intervals for  $\beta$  and  $R_0$  compared to NUTS, suggesting that ADVI may be underestimating the posterior uncertainty, as has been observed in the past. In general, the posterior estimates for  $R_0$  are in line with the estimated  $R_0$  obtained by Wearing et al. (2005). As seen from Figure 2, the deterministic model has a reasonable fit to the data but underestimates the overall uncertainty thus resulting in overly precise estimates which fail to capture the data appropriately.

Results from the stochastic model are summarized in Table 2. In addition to the parameters characterizing the transmission dynamics of the disease, we also report posterior estimates for the parameter  $\phi$  of the OU process which reflects the speed of reversion and the instantaneous variance  $\sigma^2$ . Again, the resulting 95% credible intervals from ADVI have shorter length compared to NUTS.

Table 1: HMC using 5 chains, each with iter=100500; warmup=500; thin=50; post-warmup draws per chain=2000, total post-warmup draws=10000 ; VB(meanfield) using iter=10000, tol\_rel\_obj=0.01

	Hamiltonian Monte Carlo						Variational Inference			
	Model 1			Model 2			Model 1		Model 2	
	mean	95% CI	ESS	mean	95% CI	ESS	mean	95% CI	mean	95% CI
$\beta$	1.89	1.78-2.00	9766	1.88	1.78-1.98	10166	1.89	1.86-1.93	1.87	1.84-1.90
$\gamma$	0.48	0.46-0.50	10093	0.48	0.46-0.50	9917	0.48	0.46-0.50	0.48	0.46-0.50
$s(0)$	1.00	1.00-1.00	9632	1.00	1.00-1.00	9953	1.00	1.00-1.00	1.00	1.00-1.00
$R_0$	3.93	3.67-4.22	9667	3.93	3.71-4.17	9789	3.96	3.77-4.16	3.92	3.75-4.11

Table 2: HMC using 5 chains, each with iter=100500; warmup=500; thin=50; post-warmup draws per chain=2000, total post-warmup draws=10000 ; VB(meanfield) using iter=10000, tol\_rel\_obj=0.0001

	Model 3					
	Hamiltonian Monte Carlo			Variational Inference		
	mean	95% CI	ESS	mean	95% CI	
$\beta$	2.02	1.68-2.71	9824	2.02	1.85-2.21	
$\gamma$	0.53	0.44-0.65	9965	0.55	0.45-0.66	
$s(0)$	1.00	1.00-1.00	9034	1.00	1.00-1.00	
$R_0$	3.84	2.80-5.79	9976	3.73	2.98-4.60	
$\phi$	4.34	0.46-19.19	9196	0.86	0.58-1.26	
$\sigma^2$	2.63	0.36-12.32	8599	0.70	0.45-1.02	

Table 3: Execution time (minutes)

	Model 1	Model 2	Model 3
HMC	13.63	13.59	47.68
VI	0.32	0.54	1.86

Summing up, the results of both the deterministic and the stochastic setting bring us to the preliminary conclusion that if we are interested in real-time inference both methods are feasible and efficient. In terms of computational time ADVI is extremely efficient (Table 3). As Figure 2 demonstrates (see also Appendix), adding stochasticity improves the fit to the data.

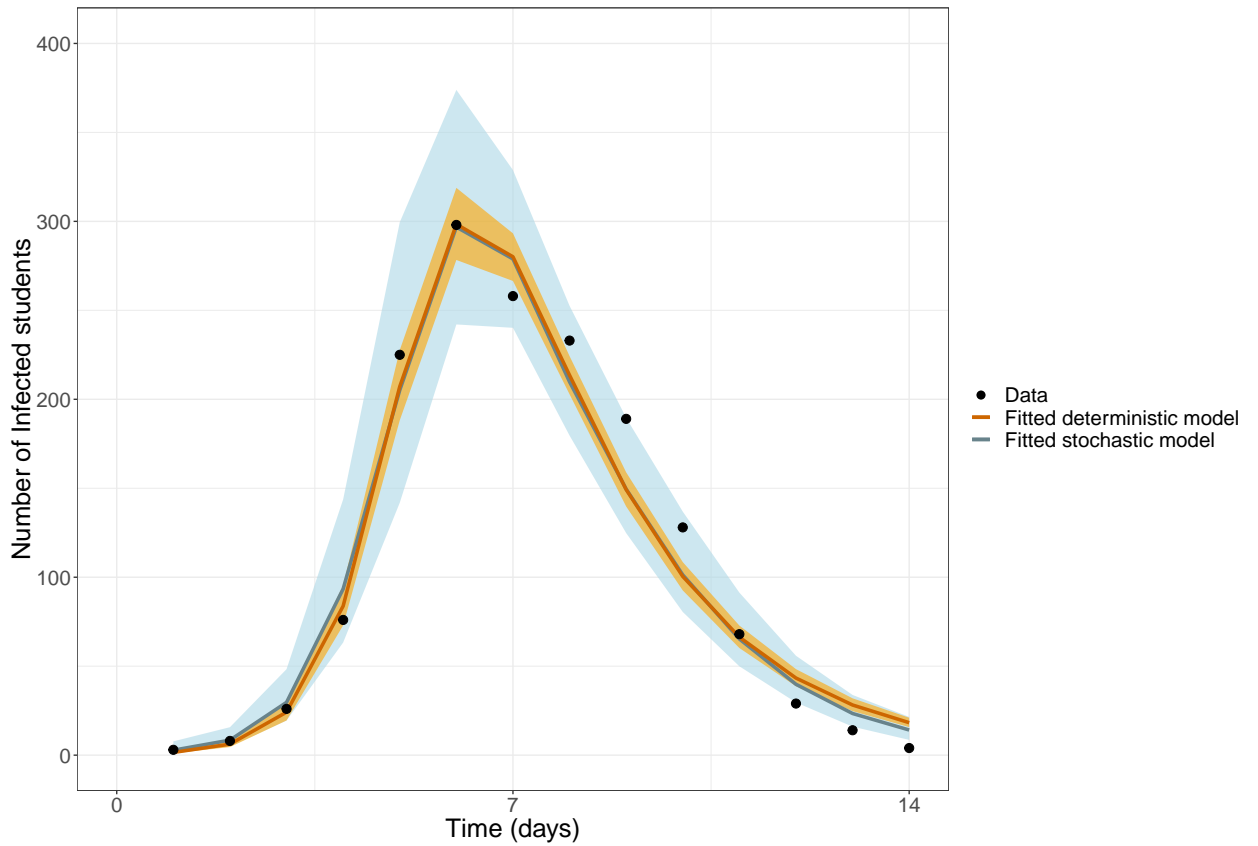


Figure 2: Model fit to the data using Hamiltonian Monte Carlo. Median and 95% Credible Interval

#### 4.3. Multistrain model

For this example we used the UK influenza data from the 2017/18 season (Public Health England). The 2017/18 season was somewhat unusual in that it had multiple influenza strains circulating. The main strain was a B strain, but a significant amount of virological samples tested positive for the H3 strain as well. Figure 3 shows the results of model fitting to the ILI GP consultations data and the virological confirmation data. The results show that the influenza strain causing the highest incidence is B, with also some ILI consultations due to infections with the H3 and H1 later in the season (top panel). Flu negative ILI is also an important fraction of the ILI consultations (yellow in the top panel), with a clear increase just before the B outbreak (11-13th week). For the virological confirmation the uncertainty

increases after week 17, this is because later in the season less virological samples are taken, resulting in much lower confidence in the actual level of positivity by strain.

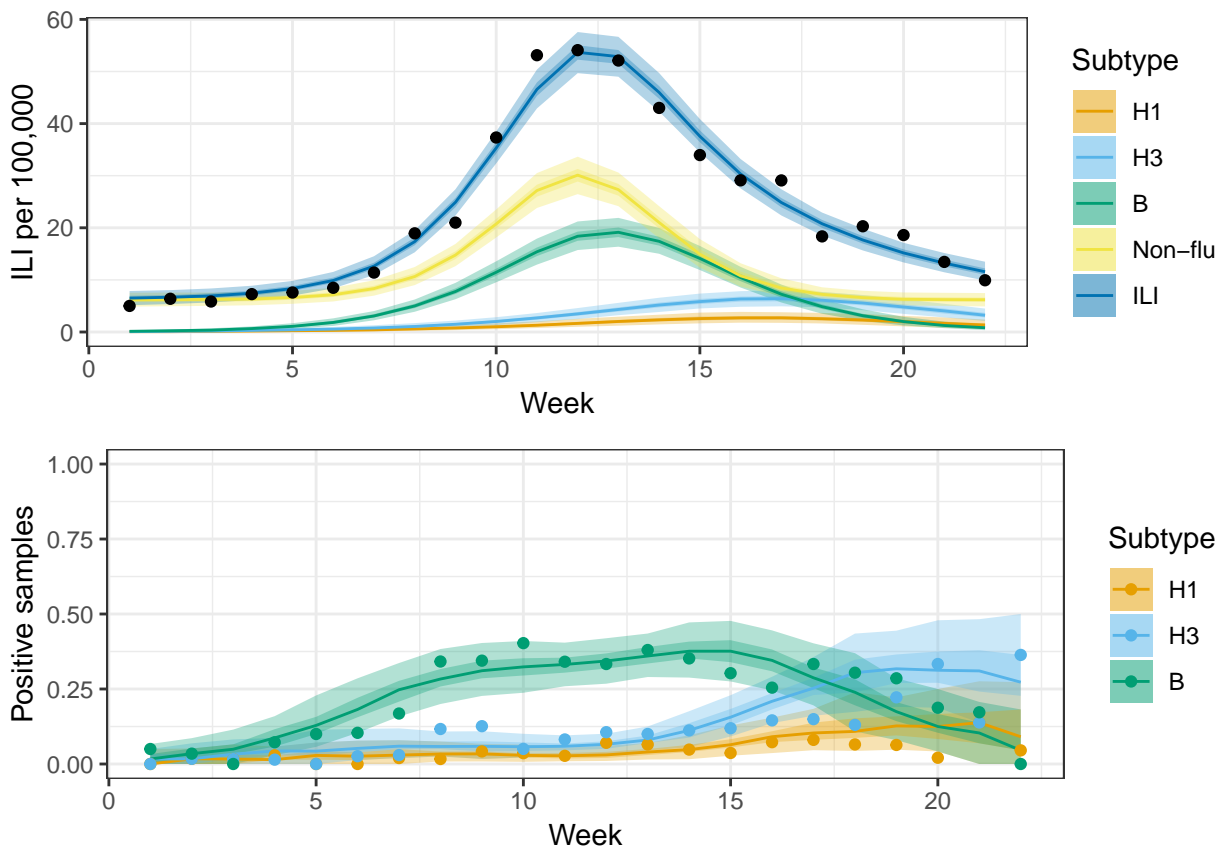


Figure 3: Model fit to the data. Top panel has the fit to the ILI consultation data (blue). Furthermore, the panel highlights the causes of ILI, i.e. by each influenza strain or other non-flu causes. The bottom panel has the fit to the virological confirmation data.

## 5. Discussion

In this paper, we summarize the basic concepts required to perform HMC and VB using Stan, in the framework of infectious disease modelling. Stan is the first general purpose statistical software allowing for relatively straightforward fitting of ODE-based models. In the presence of a system of ODEs, the respective likelihood function may have ridged regions resulting in a failure of standard regularity conditions and therefore classical likelihood or

MCMC-based inference. In these cases, we know that HMC may produce more accurate results and is readily available to epidemiologists in the form of Stan.

Stan offers flexibility in the sense that we only need to change a few lines of code in order to estimate different models either by changing the distributional assumptions or adding more components. Thus, as a generic and flexible software package along with the fact that it may perform inference fast, Stan makes real-time inference feasible.

We are not concerned in this article with detailed comparisons between HMC and ADVI algorithms as performed in Stan, since there are many factors that may affect their performance and certainly differ among different models. The chosen parameterization, priors, starting values and tuning parameters, are only a few of these factors. In general, HMC tends to be more computationally intensive than ADVI but it also offers high statistical efficiency. For epidemic models where the posterior distributions may be characterised by highly correlated parameter spaces, HMC seems to perform better than classical techniques. Currently, HMC in Stan, does not allow for discrete parameters, but they can simply be marginalized out. Finally, ADVI seems to be very promising for real-time inference but it is extremely sensitive to starting values and can underestimate posterior uncertainty. However, in practice when repeated fitting is required, say in the context of real-time inference, one may overcome this issue by a laborious initial fitting, possibly using HMC, and subsequent usage of the outcome in order to initialise the following fit.

## **Acknowledgements**

Anastasia Chatzilena states that: "Part of this research is co-financed by Greece and the European Union (European Social Fund- ESF) through the Operational Programme Human Resources Development, Education and Lifelong Learning in the context of the project Strengthening Human Resources Research Potential via Doctorate Research (MIS-5000432), implemented by the State Scholarships Foundation (IKY)"

## Appendix A. HMC-NUTS and ADVI

### Appendix A.1. HMC algorithm as performed in Stan

- **Goal:** sample from some target density  $\pi(\theta)$ , where  $\theta$  is the vector of parameters of interest.
- **Auxiliary step:**
  - Expand the original probabilistic system by introducing auxiliary momentum parameters  $p$
  - Express the target density into a joint probability distribution:

$$\pi(p, \theta) = \pi(p|\theta)\pi(\theta)$$

which can be written in terms of an invariant Hamiltonian as:

$$\pi(p, \theta) = \exp(-H(p, \theta))$$

thus,

$$\begin{aligned} H(p, \theta) &= -\log \pi(p, \theta) \\ &= -\log \pi(p|\theta) - \log \pi(\theta) \\ &\equiv \underbrace{T(p, \theta)}_{\substack{\textit{kinetic} \\ \textit{energy}}} + \underbrace{V(\theta)}_{\substack{\textit{potential} \\ \textit{energy}}} \end{aligned}$$

and the partial derivatives of the Hamiltonian determine how  $\theta$  and  $p$  change over time,  $t$ , according to Hamiltons equations:

$$\begin{aligned} \frac{d\theta}{dt} &= \frac{\partial H}{\partial p} = \frac{\partial T}{\partial p} \\ \frac{dp}{dt} &= -\frac{\partial H}{\partial \theta} = -\frac{\partial T}{\partial \theta} - \frac{\partial V}{\partial \theta} = \frac{\partial \log \pi(p|\theta)}{\partial \theta} - \frac{\partial V}{\partial \theta} = \frac{\partial \log \pi(p)}{\partial \theta} - \frac{\partial V}{\partial \theta} = -\frac{\partial V}{\partial \theta} \end{aligned}$$

since the density of momentum parameters is independent of the target density i.e.  $\log \pi(p|\theta) = \log \pi(p)$ .

- **1st step:**

Start from the current value of  $\theta$  and draw independently a value for the momentum  $p$  from a zero-mean normal distribution,

$$p \sim \text{MultiNormal}(0, \Sigma)$$

where  $\Sigma$  is the covariance matrix which is also known as the mass matrix or metric (Betancourt and Stein, 2011). The choice of  $\Sigma$  can improve the efficiency of the HMC algorithm since it can rescale the target distribution so the parameters have the same scale and rotate it appropriately so the parameters are approximately independent.

- For **L steps** alternate half-step updates of the momentum  $p$  and full-step updates of  $\theta$ :

$$p \leftarrow p - \frac{\epsilon}{2} \frac{\partial V}{\partial \theta}$$

$$\theta \leftarrow \theta + \epsilon \Sigma p$$

$$p \leftarrow p - \frac{\epsilon}{2} \frac{\partial V}{\partial \theta}$$

Therefore, each designed path of the algorithm has length  $\epsilon L$ . The optimal choice of the step size  $\epsilon$  and the number of steps  $L$  play a crucial role in the performance of HMC since paths which are too short are not able to propose distant points resulting in a random walk, while paths which are too long may eventually end at a point that has been already reached resulting in computational inefficiency. Essentially, if  $\epsilon$  is too large, the leapfrog integrators error which depends on  $\epsilon$  will be large, resulting in too many rejected proposals. If  $\epsilon$  is too small then the leapfrog integrator will have to perform too many small steps, increasing run-time. On the other hand, when choosing an  $L$  which is too small the proposed samples will be close to one another while choosing an  $L$  which is too large, the algorithm will have to do extra work at each iteration probably creating paths which retrace already sampled points.

- **Automatic Tuning of the parameters**

- Automatically select  $L$  using the no-U-turn sampler (NUTS) in each iteration (Hoffman and Gelman, 2011). NUTS uses a recursive algorithm following a doubling procedure of leapfrog steps.
- Automatically determine  $\epsilon$  during the warmup phase in order to match a target acceptance rate (Betancourt et al., 2014; Stan Development Team, 2018).
- Set  $\Sigma$  to be the identity matrix or restrict it to a diagonal matrix or estimate it using warmup samples (Stan Development Team, 2018).

*Appendix A.2. ADVI algorithm as performed in Stan*

- **Goal:** approximate some target density  $\pi(\theta)$ , where  $\theta$  is the vector of parameters of interest.

- **Variational Approximation:**

- Consider a family of approximating densities of the latent variables  $q(\theta; \phi)$ , parameterized by a vector of parameters  $\phi \in \Phi$
- Find the member of that family that minimizes the Kullback-Leibler(KL) divergence:

$$\arg \min_{\phi \in \Phi} KL(q(\theta; \phi) \parallel \pi(\theta|y))$$

$$\text{such that } \text{supp}(q(\theta; \phi)) \subseteq \text{supp}(\pi(\theta|y))$$

where  $y$  denotes the data.

- Given that the KL divergence involves the target density, its analytic form is unknown, so maximize a proxy to the KL divergence, the Evidence Lower Bound (ELBO):

$$\arg \max_{\phi \in \Phi} [\mathbb{E}_{q(\theta)}[\log \pi(y, \theta)] - \mathbb{E}_{q(\theta)}[\log q(\theta; \phi)]]$$

subject to the support constraint.

- **1st step:** Transform the parameters of interest,  $T : \theta \rightarrow \zeta$ , so that their support is in the real coordinate space i.e. define a one-to-one differentiable function,  $T : \text{supp}(\pi(\theta)) \rightarrow \mathbb{R}^\kappa$ . Then the transformed density is denoted by:

$$\begin{aligned}\pi(y, \zeta) &= \pi(y, T^{-1}(\zeta)) |\det J_{T^{-1}}(\zeta)| \\ &= \pi(y, \theta) |\det J_{T^{-1}}(\zeta)|\end{aligned}$$

where  $J_{T^{-1}}(\zeta)$  is the Jacobian of the inverse of  $T$ .

Stan supports and automatically uses a library of transformations and their corresponding Jacobians.

Also, it can be shown that the ELBO in the real coordinate space is:

$$\mathcal{L}(\phi) = \mathbb{E}_{q(\zeta; \phi)} [\log \pi(y, T^{-1}(\zeta)) + \log |\det J_{T^{-1}}(\zeta)|] - \mathbb{E}_{q(\zeta; \phi)} [\log q(\zeta; \phi)]$$

- **2nd step:** Choose the variational approximation
  - Mean-field or factorized Gaussian

$$q(\zeta; \phi) = \prod_{\kappa=1}^K \mathcal{N}(\zeta_\kappa; \mu_\kappa, \sigma_\kappa^2)$$

where  $\phi = (\mu_1, \dots, \mu_K, \sigma_1^2, \dots, \sigma_K^2)$ .

- Full-rank Gaussian

$$q(\zeta; \phi) = \mathcal{N}(\zeta; \mu, \Sigma)$$

where  $\phi = (\mu, \Sigma)$ .

- **3rd step:** Stochastic optimization in order to maximize the ELBO in the real coordinate space (Kucukelbir et al., 2017):
  - The expectations with respect to the variational parameters  $\phi$  constituting the ELBO, are unknown. Apply an elliptical standardization so the expectations do not depend on  $\phi$ .
  - Compute the gradients inside the expectation with automatic differentiation and use Monte Carlo integration to compute the expectations.
  - Given the gradients of the ELBO employ a stochastic gradient ascent algorithm

## Appendix B. Single strain deterministic and stochastic model results using ADVI

Results from ADVI both for the deterministic and the stochastic model are shown in the following figure:

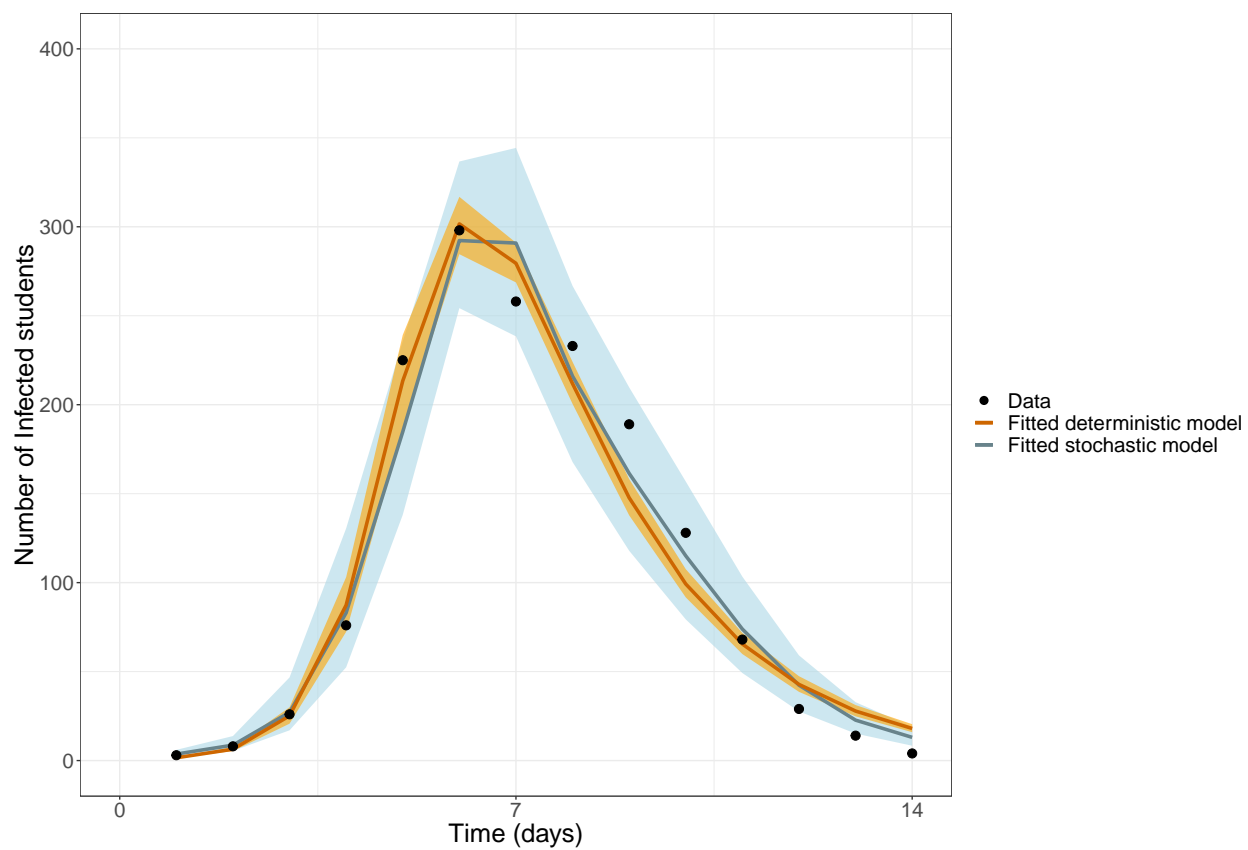


Figure B.4: Model fit to the data using ADVI. Median and 95% Credible Interval

## References

- R. M. Anderson and R. M. May. *Infectious diseases of humans: dynamics and control*. Oxford university press, 1992.
- H. Andersson and T. Britton. *Stochastic epidemic models and their statistical analysis*, volume 151. Springer Science & Business Media, 2000.
- M. Baguelin, S. Flasche, A. Camacho, N. Demiris, E. Miller, and W. J. Edmunds. Assessing optimal target populations for influenza vaccination programmes: an evidence synthesis and modelling study. *PLoS medicine*, 10(10):e1001527, 2013. doi:10.1371/journal.pmed.1001527.
- M. Betancourt. Identifying the Optimal Integration Time in Hamiltonian Monte Carlo. *arXiv e-prints*, art. arXiv:1601.00225, Jan 2016.
- M. Betancourt. A Conceptual Introduction to Hamiltonian Monte Carlo. *arXiv e-prints*, art. arXiv:1701.02434, Jan 2017.
- M. Betancourt and L. C. Stein. The Geometry of Hamiltonian Monte Carlo. *arXiv e-prints*, art. arXiv:1112.4118, Dec 2011.
- M. Betancourt, S. Byrne, S. Livingstone, M. Girolami, et al. The geometric foundations of hamiltonian monte carlo. *Bernoulli*, 23(4A):2257–2298, 2017. doi:10.3150/16-BEJ810.
- M. J. Betancourt, S. Byrne, and M. Girolami. Optimizing The Integrator Step Size for Hamiltonian Monte Carlo. *arXiv e-prints*, art. arXiv:1411.6669, Nov 2014.
- C. M. Bishop. *Pattern recognition and machine learning*. springer, 2006.
- D. M. Blei, A. Kucukelbir, and J. D. McAuliffe. Variational inference: A review for statisticians. *Journal of the American Statistical Association*, 112(518):859–877, 2017. doi:10.1080/01621459.2017.1285773.
- B. Carpenter, M. D. Hoffman, M. Brubaker, D. Lee, P. Li, and M. Betancourt. The Stan Math Library: Reverse-Mode Automatic Differentiation in C++. *arXiv e-prints*, art. arXiv:1509.07164, Sep 2015.

- B. Carpenter, A. Gelman, M. D. Hoffman, D. Lee, B. Goodrich, M. Betancourt, M. Brubaker, J. Guo, P. Li, and A. Riddell. Stan: A probabilistic programming language. *Journal of statistical software*, 76(1), 2017. doi:10.18637/jss.v076.i01.
- P. de Valpine, D. Turek, C. J. Paciorek, C. Anderson-Bergman, D. T. Lang, and R. Bodik. Programming with models: writing statistical algorithms for general model structures with nimble. *Journal of Computational and Graphical Statistics*, 26(2):403–413, 2017. doi:10.1080/10618600.2016.1172487.
- G. De Vries, T. Hillen, M. Lewis, B. SchÖnfisch, et al. *A course in mathematical biology: quantitative modeling with mathematical and computational methods*, volume 12. Siam, 2006.
- K. Dietz. The estimation of the basic reproduction number for infectious diseases. *Statistical methods in medical research*, 2(1):23–41, 1993. doi:10.1177/096228029300200103.
- D. Fleming and A. Elliot. Lessons from 40 years’ surveillance of influenza in england and wales. *Epidemiology & Infection*, 136(7):866–875, 2008. doi:10.1017/S0950268807009910.
- A. Gelman and J. Hill. *Data analysis using regression and multi-level/hierarchical models*. Cambridge university press, 2006.
- A. Gelman, H. S. Stern, J. B. Carlin, D. B. Dunson, A. Vehtari, and D. B. Rubin. *Bayesian data analysis*. Chapman and Hall/CRC, 2013.
- S. Geman and D. Geman. Stochastic relaxation, Gibbs distributions, and the Bayesian restoration of images. *IEEE Transactions on pattern analysis and machine intelligence*, (6):721–741, 1984. doi:10.1109/TPAMI.1984.4767596.
- A. Griewank and A. Walther. *Evaluating derivatives: principles and techniques of algorithmic differentiation*, volume 105. Siam, 2008.
- A. Griewank et al. On automatic differentiation. *Mathematical Programming: recent developments and applications*, 6(6):83–107, 1989.

- W. K. Hastings. Monte Carlo sampling methods using Markov chains and their applications. 1970. doi:10.1093/biomet/57.1.97.
- M. D. Hoffman and A. Gelman. The No-U-Turn Sampler: Adaptively Setting Path Lengths in Hamiltonian Monte Carlo. *arXiv e-prints*, art. arXiv:1111.4246, Nov 2011.
- M. I. Jordan, Z. Ghahramani, T. S. Jaakkola, and L. K. Saul. An introduction to variational methods for graphical models. *Machine learning*, 37(2):183–233, 1999. doi:10.1023/A:1007665907178.
- W. O. Kermack and A. G. McKendrick. A contribution to the mathematical theory of epidemics. *Proceedings of the royal society of london. Series A, Containing papers of a mathematical and physical character*, 115(772):700–721, 1927. doi:10.1098/rspa.1927.0118.
- A. Kucukelbir, R. Ranganath, A. Gelman, and D. M. Blei. Automatic Variational Inference in Stan. *arXiv e-prints*, art. arXiv:1506.03431, Jun 2015.
- A. Kucukelbir, D. Tran, R. Ranganath, A. Gelman, and D. M. Blei. Automatic differentiation variational inference. *The Journal of Machine Learning Research*, 18(1):430–474, 2017.
- D. Lunn, C. Jackson, N. Best, D. Spiegelhalter, and A. Thomas. *The BUGS book: A practical introduction to Bayesian analysis*. Chapman and Hall/CRC, 2012.
- D. J. Lunn, A. Thomas, N. Best, and D. Spiegelhalter. Winbugs—a bayesian modelling framework: concepts, structure, and extensibility. *Statistics and computing*, 10(4):325–337, 2000.
- C. Malesios, N. Demiris, K. Kalogeropoulos, and I. Ntzoufras. Bayesian epidemic models for spatially aggregated count data. *Statistics in medicine*, 36(20):3216–3230, 2017. doi:10.1002/sim.7364.
- R. McElreath. *Statistical Rethinking: A Bayesian Course with Examples in R and Stan*, volume 122. CRC Press, 2016.
- T. J. McKinley, J. V. Ross, R. Deardon, and A. R. Cook. Simulation-based bayesian inference for epidemic models. *Computational Statistics & Data Analysis*, 71:434–447, 2014. doi:10.1016/j.csda.2012.12.012.

- N. Metropolis, A. W. Rosenbluth, M. N. Rosenbluth, A. H. Teller, and E. Teller. Equation of state calculations by fast computing machines. *The journal of chemical physics*, 21(6):1087–1092, 1953. doi:10.1063/1.1699114.
- R. M. Neal. Probabilistic inference using markov chain monte carlo methods. 1993.
- R. M. Neal. MCMC using Hamiltonian dynamics. *arXiv e-prints*, art. arXiv:1206.1901, Jun 2012.
- P. D. O'Neill and G. O. Roberts. Bayesian inference for partially observed stochastic epidemics. *Journal of the Royal Statistical Society: Series A (Statistics in Society)*, 162(1):121–129, 1999. doi:10.1111/1467-985X.00125/.
- M. Plummer. JAGS Version 4.3.0 user manual. <http://mcmc-jags.sourceforge.net/>, 2017.
- M. Plummer et al. Jags: A program for analysis of bayesian graphical models using gibbs sampling. In *Proceedings of the 3rd international workshop on distributed statistical computing*, volume 124. Vienna, Austria, 2003.
- Public Health England. Surveillance of influenza and other respiratory viruses in the UK: Winter 2017 to 2018, PHE publications gateway number: 2018093.
- D. J. Spiegelhalter, K. R. Abrams, and J. P. Myles. *Bayesian approaches to clinical trials and health-care evaluation*, volume 13. John Wiley & Sons, 2004.
- Stan Development Team. Stan modeling language users guide and reference manual, version 2.18.0. <http://mc-stan.org/>, 2018.
- R. E. Turner and M. Sahani. Two problems with variational expectation maximization for time-series models. *Bayesian Time series models*, 1(3.1): 3–1, 2011. doi:10.1017/CBO9780511984679.006.
- M. J. Wainwright, M. I. Jordan, et al. Graphical models, exponential families, and variational inference. *Foundations and Trends® in Machine Learning*, 1(1–2):1–305, 2008. doi:10.1561/2200000001.

- Y. Wang and D. M. Blei. Frequentist consistency of variational bayes. *Journal of the American Statistical Association*, (just-accepted):1–85, 2018. doi:10.1080/01621459.2018.1473776.
- H. J. Wearing, P. Rohani, and M. J. Keeling. Appropriate models for the management of infectious diseases. *PLoS medicine*, 2(7):e174, 2005. doi:10.1371/journal.pmed.0020174.